Czech Technical University
Faculty of Nuclear Sciences and Physical Engineering
Department of Physics

Review of plasma parameters of the JET tokamak in various regimes of its operation

(Bachelor thesis)

Martin Kubič

Supervisor: Ing. Ivan Ďuran PhD.
Submitted: 31.7.2007

Název práce:
Srovnání parametrů plazmatu tokamaku JET v různých režimech jeho provozu

Autor: Martin Kubič

Obor: Fyzikální inženýrství

Druh práce: Bakalářská práce

Vedoucí práce: Ing. Ivan Ďuran, PhD. Ústav fyziky plazmatu AV ČR, v.v.i.

Abstrakt: Hlavní náplní tokamaku JET je v současné době připravovat operační režimy pro tokamak ITER. Hlavním cílem této bakalářské práce je porovnat podmínky na okraji plazmatu pro dva operační scénaře ITERu, ELMing H-mod a pokročilý režim s vnitřní transportní bariérou. Pro porovnání okrajového plazmatu v obou typech scénářů byla vytvořena rozsáhlá databáze tvořená řadou výstřelů a obsahující mnoho fyzikálních veličin charakterizujících okraj a centrum plazmatu tokamaku JET. Práce obsahuje úvod do fyziky magnetického udržení s důrazem na operační režimy tokamaku, popis tokamaku JET a jeho diagnostických systémů. Oba režimy jsou porovnávány z hlediska profilu hustoty a teploty plazmatu, radiačního profilu a obsahu nečistot. Bylo zjištěno, že k dosažení nízkého energetického zatížení divertoru pro pokročilé režimy tokamaku ITER je potřeba dodatečně přidávat nečistoty nebo navýšit hustotu v diverotu.

Klíčová slova: JET, ITER, pokročilé režimy, ELMing H-mode, okrajové plazma.

Title: **Review of plasma parameters of the JET tokamak in various regimes of its operation.**

Author: Martin Kubič

Abstract: Presently, one of the main responsibilities of JET tokamak is to prepare the operating regimes for ITER. The main aim of this bachelor thesis is to compare the edge conditions for two ITER candidate operating scenarios, ELMing H-mode and advanced regime with internal transport barrier. For this purpose statistical approach was chosen compiling a large number of JET edge and core plasma quantities across a large discharge database to assess the level of similarity in the edge plasmas of each type of scenario. The thesis contains a brief introduction into the physics of magnetically confined plasma with emphasis on operation of tokamak device. Overview of JET tokamak and its available diagnostics is presented. The both regimes are compared from the point of view of plasma density and temperature profiles, radiation patterns, and impurity content. It was found that for ITER advanced regimes additional extrinsic impurity seeding or further increase of density in divertor is needed to keep the power loads on divertor targets sufficiently low.

Key words: JET, ITER, advanced regimes, ELMing H-mode, edge plasma.

Acknowledgements

First of all, I would like to thank to my supervisor, Ing. Ivan Ďuran PhD., for providing excellent guidance and practical support. Moreover, he gave me an access to all important scientific literature and necessary data. I am also especially grateful to Dr. Richard Pitts, the Task Force E Leader at JET, for his valuable suggestions and help concerning data evaluation. The work was supported by project KJB100430504 of Grant Agency of Academy of Sciences of Czech Republic.

List of Abbreviations

JET	Joint European Torus
ITER	International Thermonuclear Experimental Reactor
ELM	Edge Localised Mode
ITB	Internal Transport Barrier
SOL	Scrape-Off Layer
CRPP-EPFL	Centre de Recherches en Physigue des Plasmas
	- Ecole Polytechnique Fédérale de Lausanne
UKAEA	United Kingdom Atomic Energy Authority
EFDA	European Fusion Development Agreement
ICRH	Ion Cyclotron Resonance Heating
LHCD	Lower Hybrid Current Drive
DD	Deuterium-Deuterium
DT	Deuterium-Tritium
DB	Double Barrier
GB	Gas Box
UV	UltraViolet
MHD	MagnetoHydroDynamics
ECE	Electron Cyclotron Emission
ECA	Electron Cyclotron Absorption
CXRS	Charge Exchange Recombination Spectroscopy
BES	Beam Emission Spectroscopy
LIDAR	LIght Detection And Ranging
LIF	Laser-Induced Fluorescence
LP	Langmuir Probe

Contents

Chapter 1

Basic Plasma Physics

1.1 Plasma definition

If the temperature of a gas is raised above about 10 000K virtually all of the atoms become ionised, with electrons becoming separated from their nuclei. The resulting ions and electrons then form two intermixed fluids. However, the electrostatic attraction between their positive and negative charges is so strong that only small charge imbalances are allowed. The result is that the ionised gas remains almost neutral throughout. This constitutes a fourth state of matter called a *plasma*.
For any species of atom there will be a plasma temperature above which all the atoms have lost an electron, and the gas is then said to be fully ionised. In the case of the hydrogen isotopes, hydrogen, deuterium and tritium, the atom has only one electron, and consequently they become fully ionised at a comparatively low temperature [1].
It is traditional and convenient to give plasma temperatures in electron volts (eV), or kiloelectron volts (keV). The electron volt is defined as the energy an electron is receives in falling through an electric potential of one volt. The conversion is given by 1eV $\doteq$ 11 600 K, and for present purposes it is adequate to think of 100 million degrees as 10 keV.
The Saha equation tells us the amount of ionization to be expected in a gas in thermal equilibrium:

$$\frac{n_i}{n_n} \approx 2.4 \times 10^{21} \frac{T^{3/2}}{n_i} e^{-U_i/kT} \tag{1.1}$$

where n_i and n_n are, respectively, the density of ionized atoms and of neutral atoms, T is the gas temperature in K, k is Boltzmann's constant and U_i is the ionization energy of the gas.

It is believed that 99 % of the matter in the universe is in the plasma state. Plasma can be found in the interior of the stars as well as in the interstellar space and in the core of the planets. Plasma also occurs in gas discharges ("neon light", lightning) as part of our daily live. The useful definition of plasma is the following:
A plasma is a quasineutral gas of charged a neutral particles which exhibits collective behavior.

We must now define "quasineutral" and "collective behavior":

- If the typical dimension L of a system is much larger than the Debey length λ_D (1.2). λ_D is a measure of the shielding distance or thickness of the sheath - then whenever local concentrations of charge arise or external potentials are introduced into the system, these are shielded out in a distance short compared with L, leaving the bulk of the plasma free of large electric potentials or fields.

$$\lambda_D = \left(\frac{\varepsilon_0 k T_e}{n e^2} \right)^{1/2} \tag{1.2}$$

  where ε_0 is vacuum permittivity, T is the temperature in K, k is Boltzmann's constant, n is plasma density and e is elementary charge. The plasma is "quasineutral"; that is, neutral enough so that one can take $n_i \backsimeq n_e \backsimeq n$, but not so neutral that all the interesting electromagnetic forces vanish.

- By "collective behavior" we mean motions that depend not only on local conditions but on the state of the plasma in remote regions as well. Because of collective behavior, a plasma does not tend to conform to external influences [2].

1.2 Types of plasmas

1.2.1 Astrophysical plasmas

There are a variety of astrophysical plasmas in nature (Figure 1.1). They cover a wide range of densities and temperatures. The interior of the sun and the stars consists of a very dense and very hot plasma (for Sun $T \approx$ 1,3keV) where light atomic nuclei fuse to heavier ones and release the access of binding energy according to Einsteins famous formula $E = mc^2$. The solar corona is a dilute magnetized plasma with temperature of several million degrees. The Sun emits an extremely dilute supersonic plasma, the solar wind, into its planet system. Near the earth the solar wind has $n_e \approx 5cm^{-3}$ and $T_e = 10^5 K$. Because of its high temperature, the plasma has still a high conductivity.
By interaction with the electromagnetic radiation from the Sun the atoms of the upper atmosphere become partly ionized. We call this plasma which expands from about 60 km to 2000 km altitude the ionosphere [3].

1.2.2 Laboratory plasmas

The tradition of laboratory plasma physics starts with the investigation of the weakly ionized plasmas of flames in the 18th century. Typical applications nowadays are plasma-aided welding and combustion for this type of plasma.
Since the plasma may carry an electric current, plasma discharges of various types are investigated in fundamental research and applied in industry. Low-pressure discharges like glow discharges carry small currents with cold electrodes. They serve for lightening, for gas lasers like the CO_2 laser or the HeNe laser, and for the wide-spread applications of plasma etching and deposition.
High-pressure discharges like arcs may carry larger currents and thereby attain higher

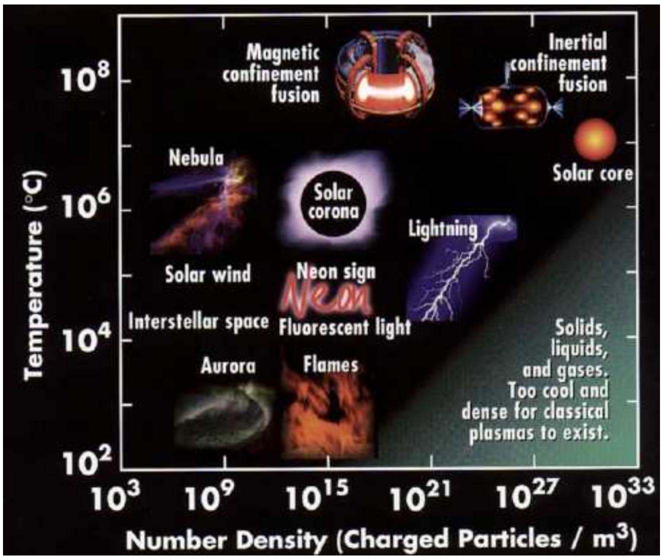

Figure 1.1: *Plasma in nature and in astrophysics.*

temperature. They may also serve for lightening like the well-known high-pressure mercury lamp, for switches, and for plasma-material processing like melting, cutting, and welding [3].
After the second world war, increasing attention was dedicated to fusion plasmas aiming for releasing of fusion energy by heating and confining ionized gas of hydrogen isotopes.

1.3 The Effect of Magnetic Field

The motion of a particle with electric charge q and mass m in electric and magnetic fields can be determined from the combined electrostatic and Lorentz force:

$$\mathbf{F} = q(\mathbf{E} + \mathbf{v} \times \mathbf{B}) \tag{1.3}$$

For $E = 0$ and a homogeneous magnetic field, the kinetic particle energy remains constant because the Lorentz force is always perpendicular to the velocity and can thus change only its direction, but not its magnitude. In a uniform magnetic field B the motion of a charged particle has two parts. Firstly, it has a circular motion perpendicular to the magnetic field, the radius of the circle being called the Larmor radius.

$$\rho_L = \frac{m_q v_\perp}{|q|B} \tag{1.4}$$

This radius increases with the energy of the particle and decreases with the strength of the magnetic field. For a typical ion in a JET plasma the Larmor radius is a few millimetres. For an electron the Larmor radius is smaller by the square root of the electron-ion mass ratio and is typically a tenth of a millimetre. Because of the opposite signs of their charges the electrons and ions circulate in opposite directions [1].
The other part of the motion is that along the magnetic field. In a uniform magnetic field the charged particle's motion parallel to the field is unaffected by the field, and the particle's "parallel velocity" is constant. When the two parts of the motion are combined we have a helical trajectory as shown in Figure 1.2.

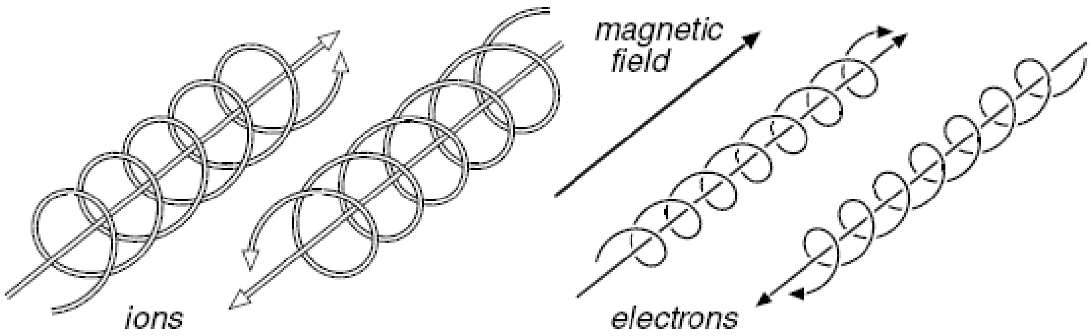

Figure 1.2: *Particle motion in uniform magnetic field.*

1.4 Particle collisions

Collisions in the plasma play an important role for all collective effects like e.g. resistivity in the plasma. When an electron collides with a neutral atom, no force is felt until the electron is close to the atom; these collisions are similar to billiard-ball collisions (Figure 1.3). However, when an electron collides with an ion, the electron is gradually deflected by the long-range Coulomb field of the ion. This force falls off comparatively slowly with distance, in fact with the inverse square of the distance between the particles. As a result of this long range interaction any given particle is colliding simultaneously with a large number of the particles. In a plasma such as that in JET each particle is simultaneously "in collision" with millions of other particles [3]. An effective collision time can be defined for each particle species as the time for the multiple collisions to produce a deflection through a large angle. The collision times depend sensitively on the plasma temperature, but taking a typical JET plasma the collision time of the electrons is a few hundred microseconds, and of the ions is tens of milliseconds. The distance travelled in this time gives a mean free path of hundreds of metres for both ions and electrons.

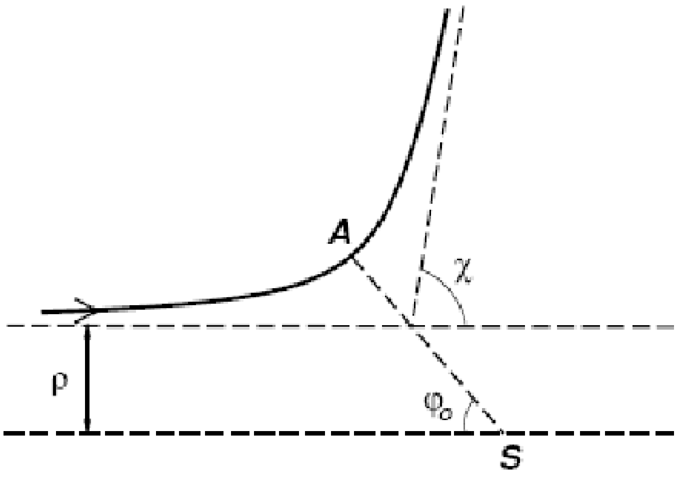

Figure 1.3: *Rutherford scattering; S is the centre of mass of the scattering partners.*

Chapter 2

Nuclear Fusion

2.1 Introduction

In astrophysics, fusion reactions power the stars and produce all but the lightest elements. Whereas the fusion of light elements in the stars releases energy, production of the heaviest elements absorbs energy, so that it can only take place in the extremely high-energy conditions of supernova explosions. In military applications, fusion of light elements provides the energy of thermonuclear explosions. If all goes well, we will manage to harness that fusion energy as a source of energy for mankind [3].
It takes considerable energy to force nuclei to fuse, even those of the lightest element, hydrogen. But the fusion of lighter nuclei, which creates a heavier nucleus and a free neutron, will generally release more energy than it took to force them together - an exothermic process that can produce self-sustaining reactions.
The energy released in most nuclear reactions is much larger than that for chemical reactions, because the binding energy that holds a nucleus together is far greater than the energy that holds electrons to a nucleus. For example, the ionization energy gained by adding an electron to a hydrogen nucleus is 13.6 eV - less than one-millionth of the 17 MeV released in the D-T (deuterium-tritium) reaction.
Any energy production from nuclear reactions is based on differences in the nuclear binding energy. Figure 2.1 shows the nuclear binding energy per nucleon (proton or neutron). It has been derived from measurements of the masses of the nuclei, when it was observed that the masses of nuclei are always smaller than the sum of the proton and neutron masses which constitute the nucleus. This mass difference corresponds to the nuclear binding energy according to Einstein's energy-mass relation $E = \Delta mc^2$.

From Figure 2.1 it is clear that there are two ways of gaining nuclear energy:

1. By transforming heavy nuclei into medium-size nuclei: this is done by fission, e.g. of uranium.

2. By fusion of light nuclei into heavier ones: in particular the fusion of hydrogen isotopes into stable helium offers the highest energy release per mass unit. Doing this in a controlled manner has been the goal of fusion research for about 40 years.

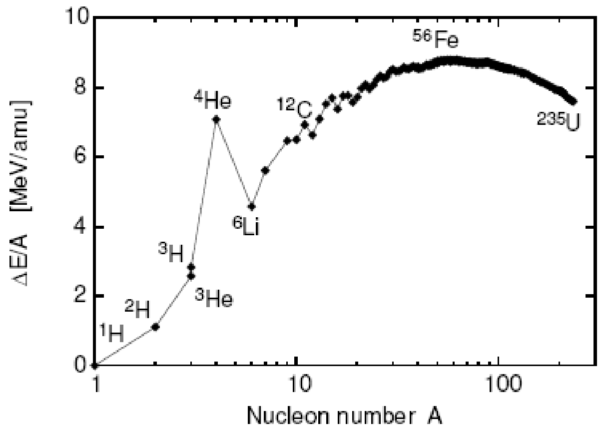

Figure 2.1: *Nuclear binding energy per nucleon as a function of the nucleon number A.*

The energy release per nucleon is of the order of 1 MeV (= 10^6 eV) for fission reactions and in the order of a few MeV for fusion reactions. This is 6-7 orders of magnitude above typical energy releases in chemical reactions, which explains the effectiveness and potential hazard of nuclear power.

2.2 Fusion on the Sun

Nuclear fusion of light elements is the source of energy produced in the stars including our Sun which maintains life on our planet. In the stars, the condition necessary for fusion as regards temperature, density and confinement time are maintained by gravity. On the Sun the main reactions are the following:

$$\begin{array}{ccc} p+p & \longrightarrow & D+e^{+}+\nu_e \\ D+p & \longrightarrow & {}^3He+\gamma \\ {}^3He+{}^3He & \longrightarrow & {}^4He+2p \end{array}$$

where p denotes a proton, D a deuteron, a heavy hydrogen isotope with one proton and one neutron, ^3He, ^4He are helium isotopes, γ stands for a high-energy photon, e^+ for a positron and ν_e for a electron neutrino [3].
Further reactions which are important at temperatures above about 1 keV, produce $^7_4$Be, $^7_3$Li, $^8_5$B and $^8_4$Be, which decays into 2$^4_2$He nuclei. Also in these reactions neutrinos are produced, however with a higher kinetic energy than those from the pp-reactions mentioned above.

2.3 Fusion on Earth

To ignite the nuclear fusion it is necessary to put together nuclei of specific light atoms close enough to overcome the strong repulsive electrostatic forces and confine them sufficiently long. Mathematically it is expressed in the Lawson criterion :

$$L = n\tau_E T_i > L_{crit} \tag{2.1}$$

where τ_E is mean value of the energy confinement time, n is plasma density and T_i is plasma ion's temperature. L_{crit} has different values for different reactions. Possible candidates for using fusion energy on earth are the following reactions (T denoting tritium, the heaviest hydrogen isotope with 2 neutrons):

$$\begin{array}{llllrllllrl}
D & + & D & \longrightarrow & {}^3He & + & n & + & 3.27MeV & (50\%) \\
D & + & D & \longrightarrow & T & + & p & + & 4.03MeV & (50\%) \\
D & + & {}^3He & \longrightarrow & {}^4He & + & p & + & 18.35MeV & \\
D & + & T & \longrightarrow & {}^4He & + & n & + & 17.59MeV & \\
p & + & {}^{11}B & \longrightarrow & 3 \cdot {}^4He & & & + & 8.7MeV &
\end{array}$$

The first four reactions (for which the cross sections are shown in Figure 2.2) can be summarized as

$$3D \longrightarrow {}^4He \;+\; p \;+\; n \quad 21.6MeV$$

and therefore rely on deuterium as fuel only. All the reaction cross sections in Figure 2.2 show a steep increase with the relative energy, but the D-T reaction

$$D \;+\; T \longrightarrow {}^4He \;+\; n \;+\; 17.59MeV$$

has by far the largest cross-section at the lowest energies. This makes the D-T fusion process the most promising candidate for an energy-producing system. To be a candidate for an energy producing system, the fusion fuel has to be sufficiently abundant. Deuterium occurs with a weight fraction of $3.3 \cdot 10^{-5}$ in water. Given the water of the oceans, the static energy range is larger than the time the sun will continue to burn.

Tritium is an unstable radioactive isotope. It decays to

$$T \longrightarrow {}^3He \;+\; e^- \;+\; \bar{\nu}_e$$

with a half-life of 12.3 years. Tritium can be produced with nuclear reactions of the neutrons from the D-T reaction and lithium:

$$\begin{array}{llllrl}
n & + & {}^6Li & \longrightarrow & {}^4He + T & +4.8MeV \\
n & + & {}^7Li & \longrightarrow & {}^4He + T + n & -2.5MeV
\end{array}$$

The ultimate fusion fuel will thus be deuterium and lithium. The latter is also very abundant and widespread in the earth's crust and even ocean water contains an average concentration of about 0.15 ppm of lithium.

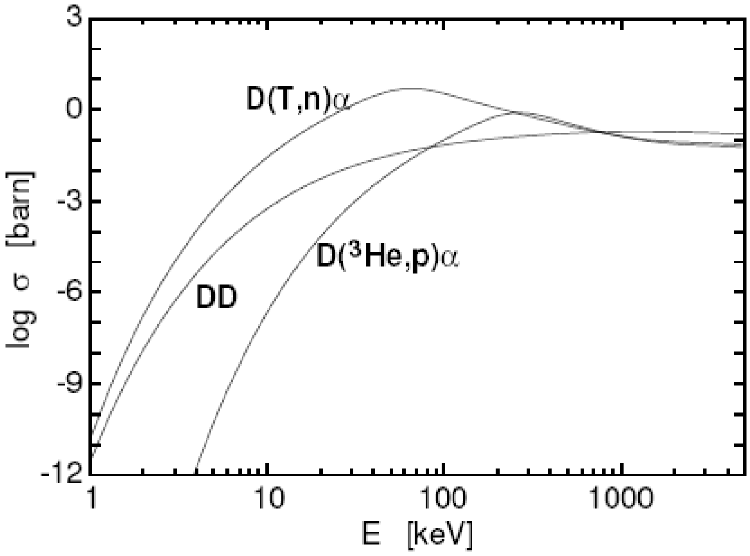

Figure 2.2: *Measured cross-sections for different fusion reactions as a function of the center of mass energy.*

2.4 Ignition

As a D-T plasma is heated to thermonuclear conditions the α-particle heating provides an increasing fraction of the total energy. When adequate confinement conditions are provided, a point is reached where the plasma temperature may be maintained against the energy losses solely by α-particle heating. The applied external heating then can be switched off and the plasma temperature is sustained by internal heating only [4]. The Lawson criterion gives for D-T reaction following condition for ignition:

$$nT\tau_i > 3.10^{20} m^{-3} keVs \tag{2.2}$$

This is a very convenient form for the ignition condition since it brings out clearly the requirements on plasma density, ion temperature, and energy confinement time. The precise value of constant in condition (2.2) depends on the profiles of n and T_i. The condition (2.2) is valid for flat profile of n and T_i.
A measure of the success in approaching reactor conditions is given by power amplification factor Q, a ratio of the thermonuclear power P_f produced to the heating power P_H supplied, that is:

$$Q = \frac{P_f}{P_H} \tag{2.3}$$

There are two ways how to reach an ignition:

1. To maximize confinement time: the hot plasma is confined by strong magnetic fields leading to maximum densities of about $1.5 \cdot 10^{20} m^{-3}$, which is $2 \cdot 10^5$ times smaller than the atom density of a gas under normal conditions. With these densities, the energy confinement time required is in the range of 2 to 4 seconds [3]. This approach is the main line in fusion research today and it is called *'magnetic confinement fusion'*

2. The other extreme is to maximize the density. This can be done by strong, symmetric heating of a small D-T pellet. The heating can be done with lasers or particle

beams and leads to ablation of some material causing implosion due to momentum conservation. It is clear that the energy confinement time is extremely short in this concept: it is the time required for the particles to leave the hot implosion center. The density required is about 1000 times the density of liquid D-T. Since it is the mass inertia which causes the finiteness of this time, this approach to fusion is often called *'inertial fusion'*.

2.5 Magnetic confinement fusion

Two different principles for twisting the magnetic field lines have been invented in the '50s and are under investigation:

- *stellarator* - The stellarator was invented in 1951 by L. Spitzer in Princeton. In a stellarator the twist of the field lines is created by external coils wound around the plasma torus, as shown in Figure 2.3. Due to these external currents the plasma shape is not circular, but shows some indentation. In this case, with four coils (neighbouring coils carry opposite current), the plasma has an oval shape. These external coils have the advantage that the current can be controlled from outside and can flow continuously (Figure 2.3 left). Nowadays such "classical" stellarators have been replaced by "modular" stellarators (Figure 2.3 right), where the planar toroidal coils and the helical coils have been replaced by one complex, but modular system of non-planar coils [3].

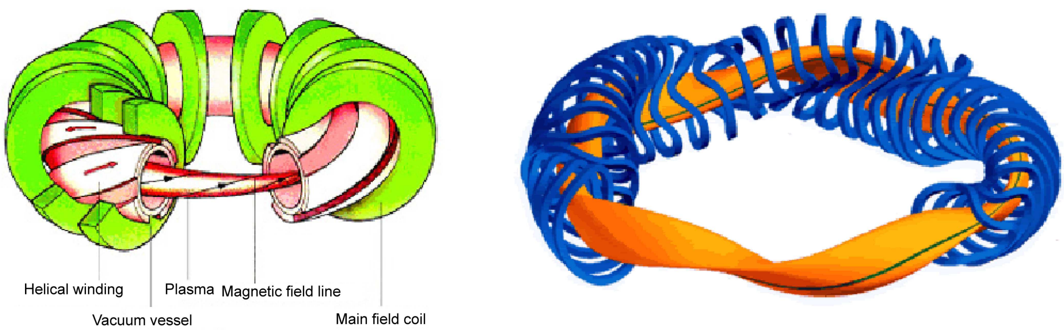

Figure 2.3: *Schematic view of a stellarator: 'Classical' stellarators (left) nowadays have been replaced by 'modular' stellarators (right).*

- *tokamak* - The tokamak was proposed by two Russian physicist, Tamm and Sakharov in 1952 and realized by Artsimovich. The word tokamak itself is derived from the Russian words for toroidal chamber with magnetic field. The tokamak concept is shown in figure 2.4. The tokamak is a toroidal confinement system in which the plasma being confined by a magnetic field. The principal magnetic field is the toroidal field. However, this field alone does not allow confinement of the plasma. In order to have an equilibrium in which the plasma pressure is balanced by the magnetic forces it is necessary also to have a poloidal magnetic field. In a tokamak this field is mainly produced by current in the plasma itself, this current is flowing in the toroidal direction. The current also serves for plasma build-up and heating.

This current is produced by induction, the plasma acting as the secondary winding of a transformer. The combination of the toroidal and poloidal field gives rise to magnetic field lines which have a helical trajectory around the torus. The toroidal magnetic field is provided by simple magnets - coils linking the plasma. The magnitude of the toroidal field is typically a few Teslas. Tokamaks have proved to be very successful in improving the desired fusion plasma conditions and the today's best experiments are based on the tokamak principle. Of course, a transformer can induce the plasma current only during a finite time. For truely continuous tokamak operation, alternative current drive methods are being developed.

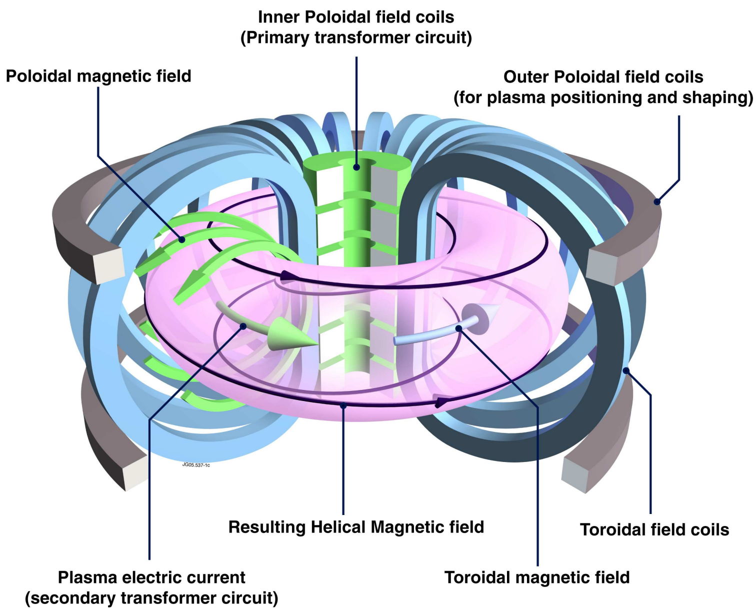

Figure 2.4: *Schematic view of a tokamak.*

Chapter 3

Joint European Torus

3.1 Introduction

The JET Joint Undertaking was established in June 1978 to construct and operate the Joint European Torus (JET), of its time the largest single project within the European nuclear fusion programme. It was coordinated by Euratom (the European Atomic Energy Community), and the JET project went on to become the flagship of the Community Fusion Programme. It started operating in 1983 and was the first fusion facility in the world to achieve a significant production of controlled fusion power (nearly 2 MW) with a Deuterium-Tritium experiment in 1991.

JET furthered fusion science well beyond the goals of the original Design Team and has evolved into a physics and technology basis for preparing for ITER, the International Thermonuclear Experimental Reactor. After 1991, JET was enhanced by the installation of a divertor to handle higher levels of exhaust power. Deuterium experiments in the ITER geometry have made essential contributions to the ITER divertor design and provided key data on heating, confinement and fuel purity. This has contributed significantly to the definition of the size, heating requirements and operating conditions of ITER [5].

During 1997 the JET operations included a three months' campaign of highly successful experiments using a range of Deuterium-Tritium fuel mixtures. The results were of major significance. JET set three new world records:

- 22 MJ of fusion energy in one pulse
- 16 MW of peak fusion power
- a 65% ratio of fusion power produced to total input power

In Spring 1998 the fully remote handling installation of an ITER-specific divertor was successfully completed on time, demonstrating another technology vital for both ITER and a future fusion power station. Experimental work continued in 1999, in particular to characterise the new divertor configuration to control impurities and plasma density and to develop Internal Transport Barrier scenarios in preparation of ITER.

The ownership of the JET Facilities was transferred to the UK Atomic Energy Authority (UKAEA), and the overall implementation and co-ordination of further scientific exploitation is now carried out under EFDA, the European Fusion Development Agreement.

3.2 Description of the JET tokamak

The toroidal component of the magnetic field on JET is generated by 32 large D-shaped coils with copper windings, which are equally spaced around the machine. The primary winding (inner poloidal field coils) of the transformer, used to induce the plasma current which generates the poloidal component, is situated at the centre of the machine. Coupling between the primary winding and the toroidal plasma, acting as the single turn secondary, is provided by the massive eight limbed transformer core. Around the outside of the machine, but within the confines of the transformer limbs, is the set of six field outer poloidal field coils used for positioning, shaping and stabilising the position of the plasma inside the vessel. During operation large forces are produced due to interactions between

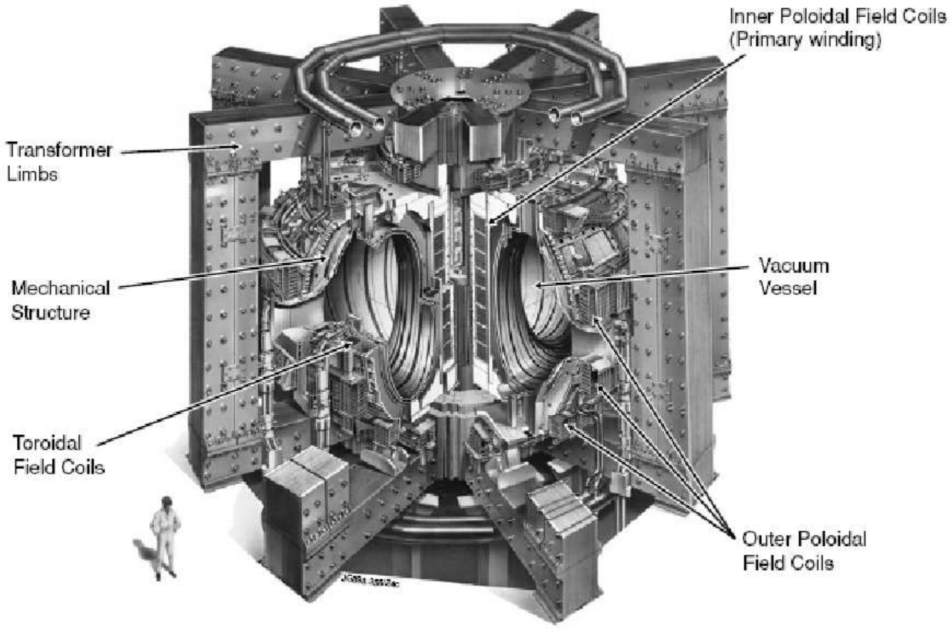

Figure 3.1: *Drawing of the JET tokamak*

the currents and magnetic fields. These forces are constrained by the mechanical structure which encloses the central components of the machine [5].
The use of transformer action for producing the large plasma current means that the JET machine operates in a pulsed mode. Pulses can be produced at a maximum rate of about one every twenty minutes, and each one can last for up to 60 seconds in duration. The plasma is enclosed within the doughnut shaped vacuum vessel which has a major radius of 2.96m and a D-shaped cross section of 4.2m by 2.5m. Figure 3.1 gives a drawing of the JET tokamak showing the general layout.

3.2.1 The Vacuum Vessel

The basic purpose of the vacuum vessel is to hold a vacuum in which the pressure is less than one millionth of atmospheric pressure. This means of course that it has to carry the force of atmospheric pressure over the whole of its surface, 10 tonnes per square metre over an area of 200 square metres. In order to cleanse the plasma-facing surface of the vessel of impurities it is designed to be baked at 500°C, and this implies the additional

Plasma major radius	2.96m
Plasma minor radius	2.10m (vertical) 1.25m (horizontal)
Flat-top pulse length	20s
Weight of the iron core	2800t
Toroidal Field Coil Power (Peak On 13s Rise)	380MW
Toroidal magnetic field (on plasma axis)	3.45T
Plasma current	3.2MA (Circular plasma) 4.8MA (D-Shape plasma)
Volt-seconds to drive plasma current	34Vs
Used additional heating power	25MW

Table 3.1: *JET parameters*

requirement that the heating and cooling has to be carried out without unacceptable stresses from expansion and contraction. The vessel is designed with a double skin to allow heating by hot gas which is passed through the interspace [1].

3.2.2 Magnetic Field Coils

The toroidal magnetic field is produced by 32 D-shaped coils enclosing the vacuum vessel and the layout of these coils is illustrated in Figure 3.2. Each coil is wound with 24 turns of copper bar and weighed 12 tonnes. The combined current carrying capacity of all the coils is 51 MA. The coils carry currents for several tens of seconds and consequently they had to be cooled using water as the coolant. The magnetic field exerts an expansive force

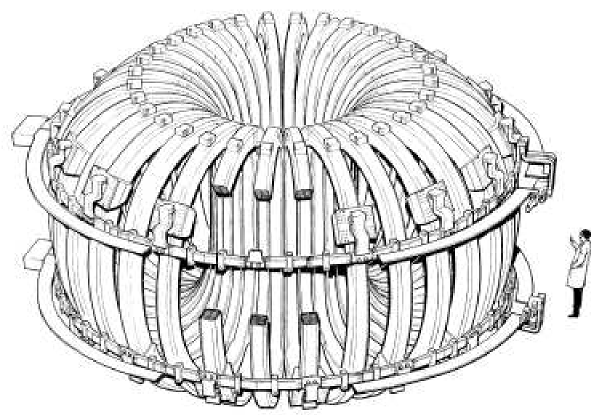

Figure 3.2: *The toroidal field coil system*

on the coils and the tensile force on each coil is up to 600 tonnes, this force being carried by the tensile strength of the copper. The total force on each coil is almost 2000 tonnes,

directed toward the major axis of the torus. A further force arises from the interaction of the currents in the coils with the poloidal magnetic field. The current in the toroidal field coils crosses the vertical component of the poloidal field in opposite directions in the upper and lower halves. This produces a twisting force which, in the JET design, is carried by an outer mechanical structure [1].
The poloidal field coils are horizontal circular coils. If these coils were placed inside the toroidal field coils the two sets of coils would be linked, with the associated problems of assembly. The poloidal field coils are therefore placed outside the toroidal field coils. The main poloidal field coil is the inner coil wound round the central column of an iron transformer core to act as the primary of the transformer. The other six coils are optimally placed to provide control of the plasma shape and position. The largest of the coils is 11 metres in diameter.

3.2.3 Power Supplies

Every individual plasma experiment at JET lasts several tens of seconds and during experimental campaigns there are some 30 pulses a day. In other words, most of the JET power consumption is concentrated in short bursts, which is quite demanding on the electricity grid and on electrical engineering in general. Moreover, even during a single pulse, the power requirements are not constant – the pulse startup (magnetic field set-up and initial plasma heating) needs more power than the sustaining phase. The toroidal field coils are the largest single load on JET. The poloidal field system, on the other hand, has complex switching and control requirements. Running a JET pulse requires around 500 MW of power, of which more than a half goes to the toroidal field coils. Around 100 MW of power is needed to run the poloidal field system (ohmic heating and plasma shaping coils) and the rest (150 MW) runs the additional heating sources (neutral beams and RF heating) [5].

3.2.4 Plasma Heating Systems

One of the main requirements for fusion is to heat the plasma particles to very high temperatures or energies. The following methods are typically used to heat the plasma:

- **Ohmic heating**: The initial heating in all tokamaks comes from the ohmic heating caused by the toroidal current. Currents up to 5 MA are induced in the JET plasma. At low temperatures ohmic heating is quite powerfull and, in large tokamaks, produces temperature of a few keV. The current inherently heats the plasma by energising plasma electrons and ions in a particular toroidal direction. A few MW of heating power is provided in this way.

- **Neutral beam heating**: A widespread technique of the additional plasma heating is based on the injection of powerful beams of neutral atoms into ohmically preheated plasma. The beam atoms carry a large uni-directional kinetic energy. In the plasma, beam atoms loose electrons due to collisions, i.e. they get ionised and as a consequence are captured by the magnetic field of tokamak. These new ions are much faster then average plasma particles. In a series of collisions, the group velocity of beam atoms is transferred into an increased mean velocity of the chaotic motion of all plasma particles. In fusion experiments, the neutral beams are usually formed by atoms of hydrogen isotopes (hydrogen, deuterium or even tritium at JET). The energy of the beam must be sufficient to reach the plasma centre - if the beam atoms were too slow, they would get ionised immediately at the plasma edge. At the same time, the beam is supposed to have enough power to deliver significant amounts of fast atoms into plasma, otherwise the heating effect would not be noticeable. At JET the beam energy is 80 or 140 keV. The total power of beam heating at JET is as much as 23 MW.

- **Radio-frequency heating**: As the plasma ions and electrons are confined to rotate around the magnetic field lines (gyro-motion) in the tokamak, electromagnetic waves of a frequency matched to the ions or electrons gyrofrequency are able to resonate or damp their wave power into the plasma particles.
  Ion cyclotron resonant heating (ICRH) is routinely applied on JET. It is resonant with the second harmonic frequency of ion gyration of main plasma ions (deuterium) or with a base frequency of gyration of minority species (tritium, helium...). The available resonant frequencies at JET are in the range of 23-57 MHz. In total, the installed power of JET ICRH system is as much as 32 MW and in practice only part of this potential can be coupled to plasma.
  There are many other resonant frequencies in tokamak plasmas but experiments have found some to be inefficient or impractical while others simply cannot penetrate through the plasma edge region. Although the lower hybrid frequency can get into the plasma, unfortunately it has an inefficient heating effect. Nevertheless another significant application of lower hybrid frequency has evolved: the corresponding lower hybrid wave can drive electric current thanks to the fact that it has an electric component parallel to magnetic field lines. At JET, *Lower Hybrid Current Drive (LHCD)* system work at frequency 3.7 GHz. The LHCD installed capacity at JET is 12 MW of additional power. Thanks to this system, off-axis electric current of several MA can be driven.

3.3 JET operating regimes

There are variety of experimental regimes of JET tokamak. The reference confinement scenario, used for extrapolation to a burning fusion plasma, is based on the H-mode which exhibits a transport barrier at the plasma edge. Confinement modes with *internal transport barriers (ITB)*, also referred to as advanced tokamak scenarios, are key to steady state operating regime of ITER. They are basically defined by the same aims namely improving confinement, stability and bootstrap current fraction [6]. The bootstrap current is associated with the trapped particles in a tokamak plasma and, therefore, it is a consequence of the inhomogeneity of the magnetic field strength. The most of the JET discharges starts with a L-mode phase with medium confinement properties and low gradients (Figure 3.3a). The L-mode is governed by a high level of turbulence which enhances the radial transport perpendicular to the magnetic field lines. The combination of sufficiently high neutral beam heating power and divertor configuration led to the discovery of a high confinement mode in the ASDEX tokamak. This H-mode is characterized by an increase of the pressure gradient at the plasma edge which is associated witch a local reduction of the turbulent transport due to shear in the $E \times B$ flow leading to a decorrelation of the underlying fluctuations.
While in L-mode the gradients are limited over the whole plasma cross section, the H-mode exhibits a region with large gradients at the edge, therefore, also termed edge transport

barrier, but a similarly flat region in the plasma core. It is evident from the pressure profile shown (Figure 3.4(b)) that in H-mode the product of pedestal pressure and plasma volume already represents large fraction of the total plasma stored energy. Following the similar considerations as for edge transport barrier, an internal transport barrier may be regarded as a region with a steep pressure gradient inside the plasma core region, as illustrated in Figure 3.4(c). Internal transport barrier can be basically defined as a region

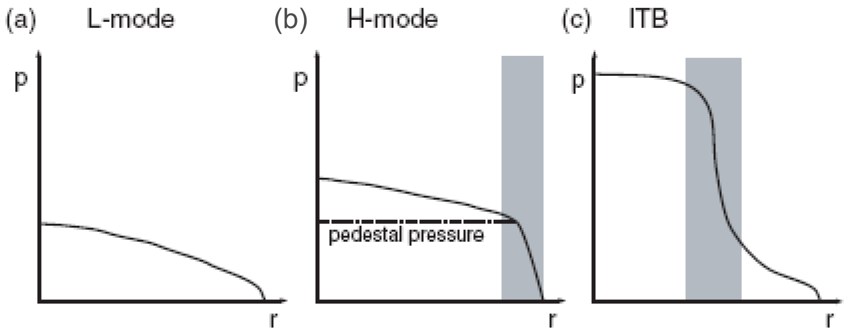

Figure 3.3: *Illustration of pressure profile observed in (a) L-mode, (b) H-mode and (c) with an internal transport barrier (ITB). The shaded areas indicate regions of reduced radial transport which in H-mode is located at the plasma edge and for an ITB in the plasma core.*

of reduced radial transport of energy or particles and hence increased pressure gradients. Usually, an ITB is postulated if at constant heating power the gradients of temperature or density increase locally above the previously observed level, which corresponds to a local reduction of the heat or particle diffusivities. Internal transport barriers arise from an influence of the magnetic shear $s = (r/q)dq/dr$ on the growth of micro-instabilities. In conventional tokamak plasmas without ITB, q increases monotonically from the center towards the edge, i.e. the magnetic shear is positive across the entire plasma radius. Only in conjuction with ITB, due to the large off-axis bootstrap current, does the q profile become non-monotonic (Figure 3.4, top right panel). It is observed that heat transport can be reduced at plasma regions with low or negative magnetic shear. In the discharges with ITB, heating power is applied early in the plasma current ramp, resulting in higher central T_e. Due to the increased resistive skin time the initial flat or slightly hollow plasma current profile remains "frozen" for the duration of the experiment.

Figure 3.4 compares profiles of the pressure, toroidal current density and safety factor q (assuming pure ohmic or pure bootstrap current) for both a "conventional" (non-ITB) and an ITB plasma. In the conventional scenario the ohmic (inductively driven) current dominates. The ohmic current density profile is fixed by the conductivity (electron temperature) profile. A sufficiently strong transport barrier can, in principle, sustain a reversed shear profile. The strong pressure gradient produced by the transport reduction creates a strong off-axis bootstrap current. The resulting non-monotonic current profile maintains the weak or negative magnetic shear profile that allows to sustain the transport barrier. A tokamak reactor with an ITB and this type of "self-generated" plasma current could be built smaller than a conventional tokamak and would allow true steady-state operation.

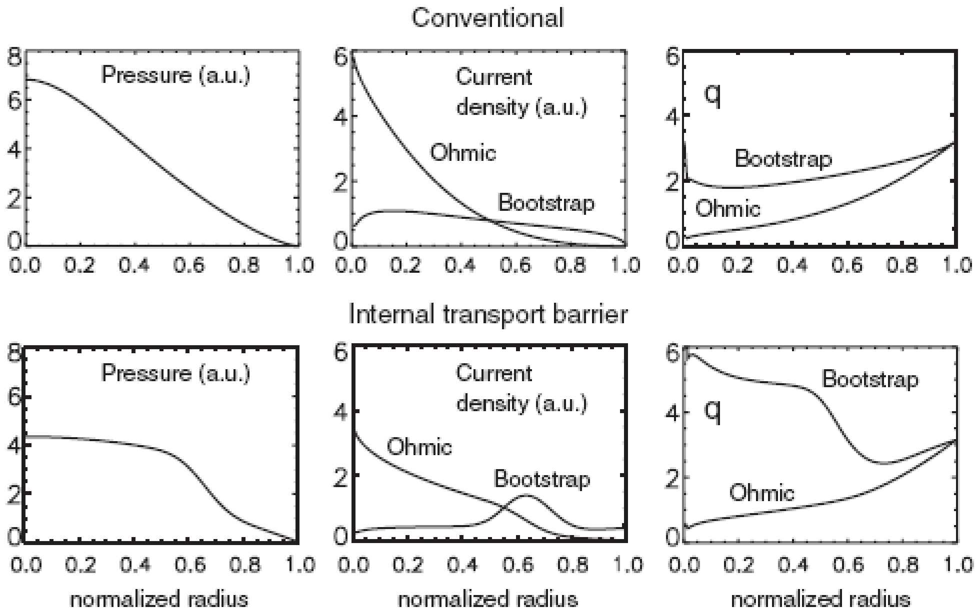

Figure 3.4: *Profiles of plasma pressure p, current density j and safety factor q comparing conventional and advanced scenarios. A conventional plasma has a monotonously rising q profile. Flat or reversed q profile can lead to a transport barrier. In an ideal advanced scenario, the resulting steep pressure gradient creates a bootstrap current that maintains the q profile non-inductively in steady state. Ohmic and bootstrap contributions to j and q are shown separately. Graphs courtesy of ASDEX Upgrade.*

Although the sustainment of the ITB was complicated by the lower H-mode threshold with tritium, the reduction in electron and ion transport seems similar in DD and DT plasmas. In fact, one of the main obstacles of extending the ITBs in JET and also in other tokamaks to power levels clearly above the H-mode threshold is the incompatibility with the large Type-I ELMs, which, although being an instability of the edge H-mode transport barrier, seem to perturb the core plasma also and thus destroy the ITB. In JET, ITBs have been combined with L- and H-mode edge conditions. The latter include edge transport barriers with both Type-III and Type-I ELMs and have been termed double transport barriers or double barrier (DB) modes. The ability of JET tokamak to form ITBs and keep the plasma edge in L-mode depends on the divertor configuration. While with the 'Mark-IIa' divertor ITBs with L-mode edge plasmas were obtained regularly, this was not possible anymore with the more closed 'Mark-IIGB' ('GB' for gas box) divertor, where the edge, on increasing the heating power, immediately went into H-mode.

Chapter 4

Plasma Diagnostics

4.1 Introduction

Plasma physics is currently one of the most active subdisciplines of physics. Measurements of the parameters of laboratory plasmas, termed *plasma diagnostics*, are based on a wide variety of characteristic plasma phenomena. Understanding these phenomena allows standard techniques to be applied and interpreted correctly and also forms the basis of innovation. The overall objective of plasma diagnostics is to deduce information about the state of the plasma from practical observations of physical processes and their effects. Many different techniques are being used for measuring the spatial profiles and evolution of various plasma parameters. Although most of them are already well established, plasma diagnostics is still a very challenging discipline [7].
Tokamak JET has one of the most complete set of diagnostics for reactor grade plasmas in the world, with unique capabilities in measuring the thermonuclear fusion products, i.e. the fast neutrons, gamma rays and alpha particles (both confined and lost). It is the only tokamak facility that can use all hydrogen isotopes. Absolutely unique diagnostics are also required to measure the plasma isotopic composition. Other major goals of the JET diagnostics are common to other big fusion experiments: to determine plasma temperature and density, to measure plasma particle and radiation losses, to find out the magnetic topology and to observe plasma flows and fluctuations. The specificity of JET, in this case, consists of providing conditions for these measurements that are closest to a reactor environment. Below are a few important examples of the diagnostics methods applied at JET.

4.2 Categorization of plasma diagnostics

Plasma diagnostics can be categorized in various ways. In gross lines the various plasma diagnostics can be categorized in seven subgroups (magnetics, probes, spectroscopy (visible, UV, x-ray), mm- and sub-mm diagnostics, laser-aided diagnostics, particle diagnostics, and fusion product diagnostics). Temperatures in magnetic confinement devices may range from several eV in the scrape-off layer to tens of keV in the plasma core. Also the density range covers many decades from 10^{17}–$10^{21} m^{-3}$. Therefore, the diagnostic systems should preferably have a large dynamic range [8]. Because of the high temperatures and densities of presentday fusion plasmas, only diagnostic techniques that have no physical contact with the plasma can be employed (except for probes that are usually applied at the very plasma edge). Hence, the plasma must be diagnosed either by analyzing the radiation and particles emitted by the plasma itself (*passive diagnostics*) or by probing the plasma with electromagnetic waves or particle beams (*active diagnostics*). Especially in the larger fusion devices it is important that the diagnostics are insensitive to the hostile environment (e.g., high heat loads, neutron and gamma - radiation), which can lead to thermal and mechanical stresses as well as to a large number of radiation-induced effects. Moreover, they must be well screened for the high electromagnetic stray fields around these devices. In the following sections the various groups of diagnostics will be shortly discussed but it is certainly not the intention to give an exhaustive overview of all possible diagnostics.

4.2.1 Magnetics

Magnetic diagnostics operate in the frequency range from about 100 Hz up to several MHz. This is the frequency range in which many typical plasma processes are active, like MHD (MagnetoHydroDynamics) instabilities. Magnetic diagnostics are indispensable for the operation of magnetic confinement devices. They are used for measuring basic plasma parameters as the plasma current, position, shape and pressure, as well as for detecting plasma instabilities. Magnetic diagnostics make use of the electromagnetic waves emitted by the plasma and are therefore passive.
The simplest magnetic diagnostic is the *pick-up coil* whose integrated voltage output is a measure for the magnetic field strength. Combinations of pick-up coils are generally used to determine the plasma position and shape.
Another very basic magnetic diagnostic is the *Rogowski coil*, which is a solenoid wound in such a way around a poloidal cross section of the plasma that its integrated output voltage is proportional to the plasma current enclosed by the coil. Voltage loops are used to measure the loop voltage and, hence, if the plasma current is known from a Rogowski coil, also the ohmic input power. *Diamagnetic loops* are used to yield a value for the total energy content of the plasma (i.e. plasma pressure).

4.2.2 Microwave diagnostics

Microwave diagnostics (also often indicated by mm and sub-mm diagnostics) are in the frequency range from 1 GHz – 3 THz. Many powerful and widely applied diagnostics like reflectometry, electron cyclotron emission (ECE) and absorption (ECA) and interferometry/polarimetry belong to this group. Apart from ECE all diagnostics in this group are active. Interferometry/polarimetry is often regarded as a laser-aided diagnostic. In *reflectometry*, a wave with a frequency below the cutoff frequency is launched into the plasma. As a consequence the wave will be reflected from the so-called critical density layer. One can deduce the position of that layer by measuring the phase shift of the probing wave with respect to a reference wave or by measuring the time-of flight of a short microwave pulse to the reflecting layer and back. Multiple-fixed or swept frequency systems are employed for measuring the electron density profile.
Interferometry is based on the phase shift that a wave experiences upon passage through the plasma with respect to the vacuum situation. The frequency is above the cutoff fre-

quency and is a trade-off between maximum phase shift and minimum disturbance by vibrations and refraction. By also measuring changes in the plane of polarization of the wave it is possible to extract information about the internal magnetic field and, so, the current density in the plasma.
Electron cyclotron emission (ECE) is based on the cyclotron radiation emitted by the electrons during their gyration around the magnetic field lines. The frequency depends on the strength of the magnetic field and, hence, on the position in the plasma. The intensity of the radiation is for optically thick plasmas proportional to the local electron temperature.

4.2.3 Spectroscopy

Spectroscopic diagnostics are employed from very long to very short wavelengths. The full range runs from approximately 10 m (ion cyclotron emission spectroscopy) down to 10 pm (hard x-ray spectroscopy). Apart from charge exchange recombination and beam emission spectroscopy (CXRS and BES) all spectroscopic diagnostics are passive.
Spectroscopy in the visible, VUV, XUV and soft x-ray spectral regions can give a wealth of information on the atomic (ionic) processes in the plasma. The plasma emission in these spectral regions consists of continuum radiation and line radiation. The intensity of the continuum radiation is a complicated function of the electron temperature and density and the impurity content. When knowledge is obtained about the electron temperature and density from other diagnostics, the impurity enhancement factor (related to Z_{eff}) may be obtained from measurements in line-free spectral regions. Measurements of line intensities, broadening and shifts can yield valuable information on ion densities, temperatures and plasma rotation. For many of these measurements a good spectral resolution is of prime importance.

4.2.4 Laser-aided diagnostics

Very similar to spectroscopy, laser-aided diagnostics are applied in wide wavelength range.
Incoherent Thomson scattering is being applied at nearly every confinement device. It is a very powerful method to measure very localized values (or profiles) of the electron temperature and density. Ruby and Nd:YAG lasers are most often applied for this purpose.
In JET, a special configuration of Thomson scattering is used and it is called *LIDAR*. LIDAR (LIght Detection And Ranging) is an ingenious system designed for, and introduced on JET to measure the electron temperature and density. Its name is a variant on RADAR, with which radio pulses are sent out, and reflections from objects along the path of the pulse are used for detection and range finding. With the JET system light pulses replace the radio pulses. The method is based on Thomson scattering. When light is passed through a plasma the electrons are accelerated by the oscillating electric field of the light wave and this acceleration causes them to emit radiation - so-called scattered radiation. However, because of their thermal motion the electrons pass through the wave and see a different frequency from that of the original wave. This causes a change in the frequency they emit, and because the change depends on the electron temperature analysis of the scattered radiation can give this temperature. The amount of scattering naturally depends on the number of scatterers, and so Thomson scattering is also used to measure the electron density. Thomson scattering measurements normally give results for a single point in the plasma. The clever idea with LIDAR is that the laser-produced

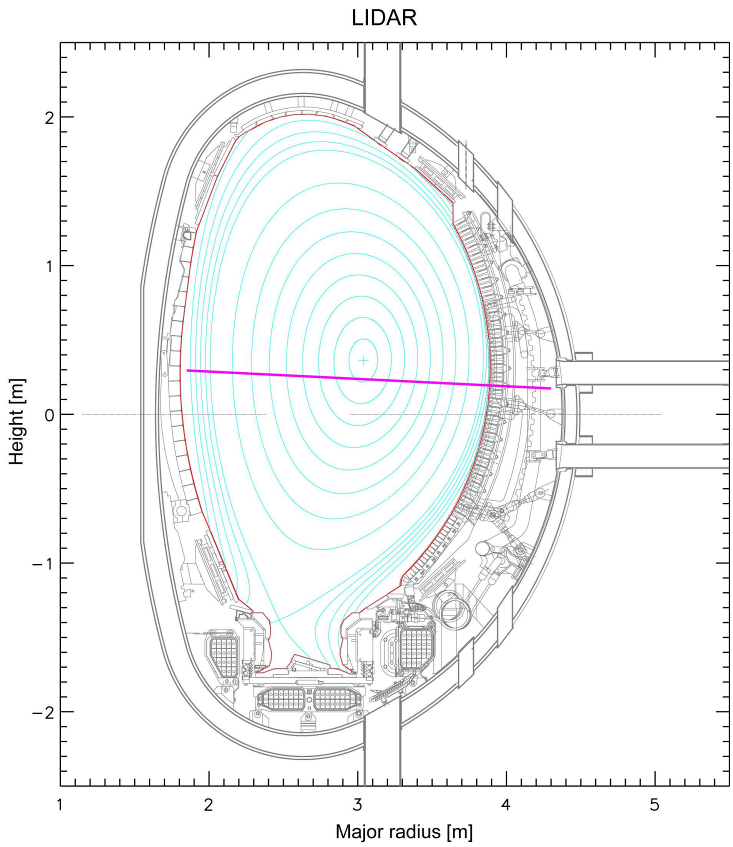

Figure 4.1: *Layout of core LIDAR system on JET. The sight line is shown by violet colour.*

light pulses are so short that they move across the plasma like bullets. This means that the measurements made at any instant correspond to the temperature and density of the electrons at the position of the pulse from which the detected scattered light was emitted. As a result, a space resolved measurement is obtained with a single laser pulse.
Two such LIDAR diagnostics run at JET - the "core" system looks at the bulk of the plasma (Figure 4.1) and the "divertor" system looks at the plasma edge. For Core LIDAR it is used a 1 J ruby laser (wavelength 694 nm) as the light source pulsed at four times a second and for a detection there is six microchannel plate photomultipliers (rise time 0.3 ns) each connected to fast data storage [5]. A second LIDAR system, the Divertor diagnostic, operates on the same principle but has a 3 J laser with a pulse repetition rate of 1 Hz. It is used four photomultipliers and detection channels.
With *laser-induced fluorescence (LIF)* transitions are induced between excited states of certain ion species. Often dye lasers are employed to tune to the specific wavelength of the transition. The induced radiation yields information on the impurity ion densities in the plasma.

4.2.5 Probes

Probes are active diagnostics in direct contact with the plasma. Therefore, they can only be applied at very plasma edge. The most well known is the *Langmuir probe*. Langmuir probes (LP) provide reliable electron temperature and density measurement in relatively cool, low-density plasmas. The probe itself is a small metal electrode - cylindrical, spherical or in the shape of a disk - inserted into the plasma. The sheath that envelops the probe shields the plasma from the probe potential. The essence of the Langmuir probe technique is to monitor the current to the probe as the probe voltage changes. The ideal I-V characteristic of such a single probe is shown in Figure 4.2. If we assume that the current drawn by the probe from the plasma is positive, when the probe bias V is very negative with respect to the plasma potential, V_p, the electric field around the probe will prevent all but the most energetic electrons from reaching the probe, effectively reducing the electron current to zero. The current collected by the probe will then be entirely due to positive ions, since these encounter only an attracting field. This current is called the 'ion-saturation current' I_{is}. As the probe bias is increased, the number of electrons which

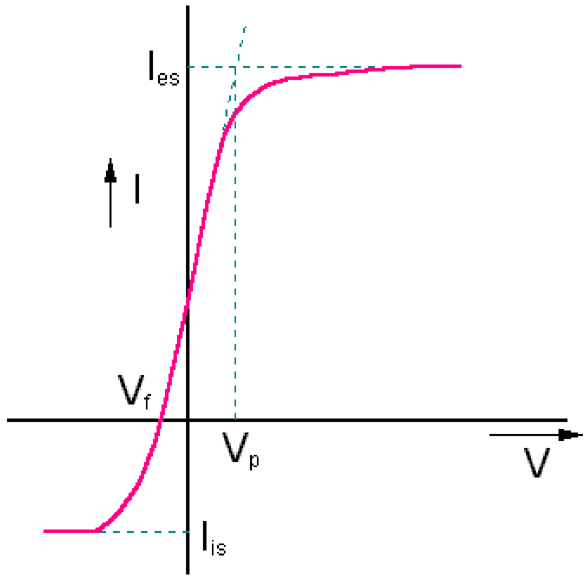

Figure 4.2: *I-V characteristic of an idealized Langmuir probe.*

is able to overcome the repulsive electric field and so contribute a negative current increases exponentially. Eventually the electron current collected is equal to -I_{is}, so that the total current is zero. At this point the floating potential V_f is reached. Further increase of the probe bias to V_p allows the electron current to totally dominate the ion current. At V_p, electrons are unrestricted from being collected by the probe. Any further increase in bias will simply add energy to the electrons, not the current drawn. Hence the term 'electron-saturation current' I_{es}. Note that this is the ideal I-V characteristics, ignoring the 'disturbing' processes such as bombardment of the probe by high energy electrons, emission of secondary electrons from the probe, and the probe etching away.
Currently there are installed 59 divertor Langmuir probes at 28 poloidal locations. They are mounted in the toroidal gaps between divertor tiles on JET tokamak. Ten of LPs have two additional pins in separate toroidal location providing a triple probe arrangement. Probes are mounted at three toroidal locations which are indexed A, B, C. Triple probes measure T_e, particle and heat fluxes with time resolution dt = 0,1 ms (single probes with 5 ms) The layout of Langmuir probes in divertor region is shown in Figure 4.3.
Bolometers are used to measure the radiation losses from the plasma in a wide wavelength range. Bolometers are also sensitive to particle losses. Wide-angle bolometers yield a value for the total radiation losses from the plasma. A bolometer is just a tiny

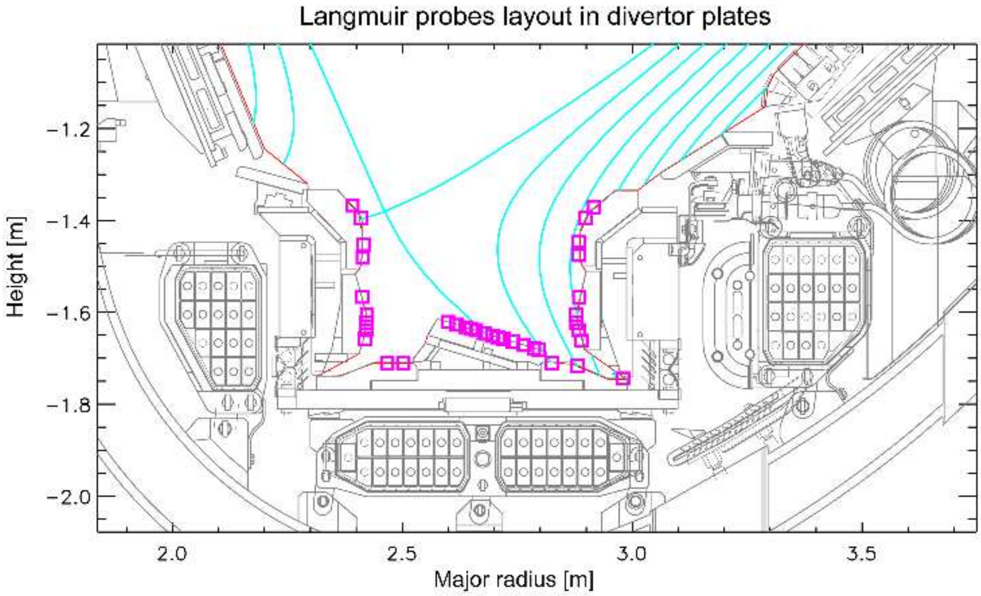

Figure 4.3: *Langmuir probes layout in divertor region.*

piece of metal with precisely defined thermal properties that heats up due to plasma radiation. The radiation comes through a narrow slit (pinhole) that defines a "viewing line" of each bolometer. Plasma radiation losses along the viewing line are then derived from the increase in the bolometer temperature. With a sufficient number of viewing lines (i.e. with a set of suitably positioned bolometers) it is possible to find out the radiation emissivity pattern of plasma cross-section. The process of calculating cross-section patterns from viewing line projections is commonly knows as tomography.

4.2.6 Particle diagnostics

Particle diagnostics are in the 10 eV - 1 MeV working range. *Neutral particle analysis (NPA)* is in essence a passive diagnostic. In the very low energy range (up to 0.5 keV) time-of-flight analyzers are often applied to measure the energy spectrum of neutral particles escaping from the plasma. This type of instrument is especially sensitive to atomic processes in the edge of the plasma. NPA at higher energies (1 - 10 keV) is used to diagnose the temperature of hydrogenic ion species in the plasma core and is employed for studying fast ion populations. In large confinement devices the number of neutral atoms emitted by the plasma core is dominated by particles emitted in copious amounts from the edge.
Charge exchange recombination spectroscopy (CXRS) is a hybrid of a particle and a spectroscopy diagnostic. This very powerful diagnostic can yield information on the impurity ion temperature, density and rotation but also on the electron density fluctuations and internal magnetic field.

4.2.7 Fusion product diagnostics

Most fusion product diagnostics are based on the passive energy analysis of particles that are resulting from fusion reactions (e.g. tritium, protons, ^{3}He, neutrons and gammas). The neutron production rate strongly depends on the ion temperature. A measurement of the neutron fluency therefore gives a first order estimate of the ion temperature. When the neutron fluency is measured along a number of well-collimated chords, the neutron birth profile and, hence, the ion temperature profile may be obtained. A problem in the interpretation of the neutron measurements is the large background of neutrons, which are generated by other processes.

4.3 Diagnostics for future devices

The next step of fusion devices, that will be operated close to ignited conditions, like ITER, will have a large influence on the field of plasma diagnostics. Diagnosticians will be facing many new problems. Firstly, the diagnostic access will be strongly limited because a large number of ports are needed to facilitate machine systems (like heating systems, robot arms for remote handling). In other words many different diagnostics have to be integrated into only a limited number of diagnostic ports. Secondly, diagnostic components that are close to the plasma are exposed to high heat fluxes as well as to high background of neutron and gamma radiation. Extensive R&D is needed to find proper solutions for the various radiation-induced effects. Thirdly, the diagnostics should be tritium compatible implying that devices must be build up in as modular way such that parts of it can be removed by remote control. Finally, the diagnostics should be reliable, also during the (quasi-) continuous operation of ITER when discharges with duration of up to 1000 s will be made.

Diagnosing fusion plasmas involves many of the most advanced measurement techniques of physics and electronic engineering. There are more than fifty different approaches applied at JET and this explains why hundreds of scientists worldwide are so interested about the performance of JET diagnostics. Nuclear fusion in general and JET in particular are the main driving forces behind the development of specific measuring techniques like fast neutron/gamma spectrometry and high energy active spectroscopy. Moreover, notice that the diagnostics of a fusion plasma operate on a quite realistic scale. Therefore, these measuring techniques can be relevant for practical applications and can potentially create interesting spin-offs.

Chapter 5

MDB database

5.1 Introduction

At JET, signals from all diagnostic systems are digitised and stored in a central database. The sampling frequencies depend on the requirements and abilities of individual diagnostics and vary from a few measurements per second up to about one million per second. In total, more than one billion readings of diagnostic data are recorded per JET pulse, each with 12 or 16 bits resolution. In other words, every JET pulse produces almost 2 GBytes of raw diagnostics data, so that as much as 50 GBytes are stored daily. Most of the data need further processing - this is done automatically where possible by dedicated computer codes, but in many cases human intervention and/or data validation is required. The processed data are stored separately from raw data. All data are accessible to all scientists on the JET site and, moreover, any scientist from any EFDA Association can work with the data from his home institute via the technique of Remote Access. Many Associations and Contractors continue to develop new diagnostics for JET or upgrade the present ones. At the same time, JET serves as a unique test bed for the development of diagnostics for the future fusion reactor machine, the ITER.

5.2 Description of MDB database

A database built with TCV MDB tool is most commonly a set of very interesting quantities (variables) taken for very interesting shots at very interesting times (samples). It can be seen as a table in which each column represents a variables and each row a sample. The samples are defined by one or more key variables, SHOT and TIME is the example. Their list is given in the manual entry file or *man* file, one of the three files constituting a database. The list of variables together with the definition of their properties is given in the variable description file or *mdb* file. These properties specify where the value of the variable for each sample comes from (in this case it is a manual entry entered in the man file) and how the sample time is selected on a time signal. The variables themselves are stored as MATLAB variables with the same name in a *mat* file forming the data file.
The *man* file contains the value for variables defined as key or manual entry by the method variable property. It is usually used to define the sample set through key variables, such

as the experimental campaign number, the shot number or the time slice and optionally to assign additional manual variables. It is an ascii file with the extension .man or a mat file with the extension .mat. Since interpreting an ascii file with a large number of samples takes time, a compiled man file with extension .manc will automatically be created and used if the ascii file has not been modified meanwhile.
The *mdb* file contains the description of the database variables. Its extension is usually .mdb. The *method* property indicates what is the information source for filling the samples and optionally how the expression property must be interpreted. By expression *method = key* is understood that the sample values for this variable must be also in the manual entry file. In addition the variables with a key method are used by MDB to distinguish different samples and their combination must be different for each sample. The most common case is to mark the shot number and the sample time as key variables.
The *selection* property specifies how the signal sample should be chosen to represent the value of this variable at a the sample time given by the TIME variable. Selection '*near*' means the following: if the processing property is empty, the signal sample at the sample time if it exists or the nearest one is selected. But the sample selection is limited on a time window centered around the sample time given by the window property. On the other hand, if a *processing* is specified, it applies on a time window centered around the sample time.
The property *processing* allows to fit a polynomial of a specified order to the signal samples contained in the time window whose length is given by the window *property.* This window is either before (*prev*), centered around (*near*) or after (*next*) the sample time, according to the selection *property.* The sample value is then that of the fitted polynomial at the sample time. For the data processing I used the mdb setting '*processing=poly0*' which calculates a mean value of the signal samples inside the time window. The comparison of using '*selection=near*' and '*processing=poly0*' for forming the database is mentioned in the following section and shown in Figure 5.1.
The data file is a *mat file* that contains the database variables themselves. For each MDB database variable, there is a Matlab variable with the same name. This is a 2-D array, numeric or a character string with always the same first dimension, so that sample number runs along this dimension. For 2-D signal there is an additional Matlab variable whose name is the name of the variable followed by an underscore. In this variable the profile of appropriate quantity is saved.

5.3 Demonstration of MDB tool data processing on JET

An example of raw data processing using MDB tool on JET is demonstrate in this section. We chose for processing the data from measurement of minor radius. For selecting the specific time value in man file, it is necessary to take into account only the times, in which the main plasma parameters are stable or do not vary too much. Plasma current, additional heating and plasma shape and other plasma properties were manually inspected for each shots and only the time instances, where these parameters are stable were included into the MDB database. The .mdb file includes in the database by default the data point nearest to the selected time. But, by using a 'processing=poly0' setting within the .mdb file, the mean values from a window of width (-0.25 + t, t + 0.25), where t denotes the specified time, are saved. This setting is more appropriate for our purposes. Figure 5.1

shows the difference between the MDB output with property 'processing=poly0' (blue circle) and without (red circle). The straight line indicates the time specified in man file for which the value of minor radius is evaluated. In this case the time is t = 5s. The dashed lines then enclose the time window of width 0.5s. For demonstration we used data from shot #67890. From Figure 5.1 it is evident that the using of property 'processing=poly0' is necessary to include mean values (within the specified time window) of the variables into the MDB database.

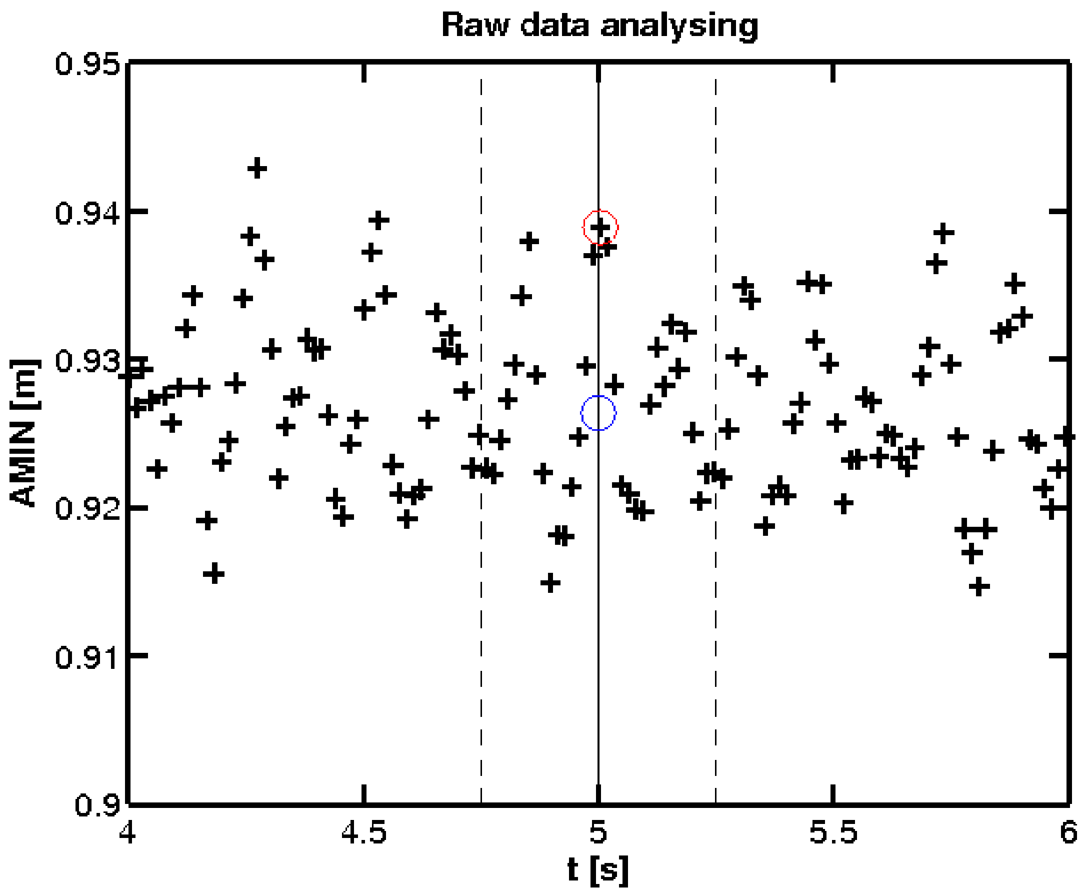

Figure 5.1: *Demonstration of data processing. The raw data are marked with +. The straight line specifies the time, in which the raw data are to be evaluated and the dashed lines enclose the time window, in which the data are processed. The output obtained with mdb settings 'selection = near' is shown by ◯ while in addition the output evaluated with mdb settings 'processing=poly0' is marked by ◯ .*

Chapter 6

Results

The reference confinement scenario, used for extrapolation to a burning fusion plasma, is based on the ELMing H-mode. Confinement modes with internal transport barriers (ITB), also referred to as advanced tokamak scenarios, are the key to non-inductive, steady-state operation in future devices and are being also developed as ITER candidate scenarios. The development of discharge scenarios with weak and strong internal transport barriers (ITB) is also one of the primary goals of research at JET (undertaken by the Scenario 2, or S2 Task Force). Although similar experiments are performed on many other tokamaks, there has never been a systematic attempt to compare the edge conditions in these advanced scenarios with those of the ELMing H-mode plasmas (studied by the Scenario 1, or S1 Task Force at JET) which will be the base-line Q_{DT} =10 scenario on ITER and which has been extensively studied with respect to edge physics. Two types of study are possible: the detailed investigation of individual discharges (from S1 and S2), including numerical fluid code modelling and a statistical approach in which a large number of edge and core plasma quantities are compared across a large discharge database to assess the level of similarity in the edge plasma of each type of scenario. We have begun by following the latter, statistical approach, compiling a database of more than 80 relevant quantities which characterize plasma geometry, basic plasma parameters including profiles of electron temperature T_e , density n_e, ion temperature T_i and all edge and scrape-off layer (SOL) properties which are currently measured on JET.
I analyzed several physical quantities of JET tokamak measured both in S1 and S2 regimes. In order to get clearer pictures, I initially build a small database containing only 33 following shots.

- ***S1 regime*** (23 discharges): 70236-70239, 70241-70243, 70245-70247, 70540-70542, 70544-70553
- ***S2 regime*** (10 discharges): 69987, 70274, 70275, 70292, 70300, 70333, 70355, 70358, 70361, 70362.

These S1 shots were performed during two experimental sessions Divertor geometry studies - ITER like on 9.3.2007 and on 26.3.2007. The first are characterized by high plasma current of 2.5 MA. The latter session is characterized by low NBI and ICRH heating of total power $\backsim$ 9 MW. The S2 shots are characterized by non external seeding. The MDB database for these shots was compiled with the following settings: window=0.5, selection='near', processing='poly0'. Only the times, in which the basic plasma parameters are stable over the MDB time window of 0.5s, were selected. For this purpose, the each shot was manually inspected using JET remote access tools and specially developed Matlab program.

6.1 Plasma shape

The Figure 6.1 shows the examples of geometry (separatrix position) of both S1 (blue line) and S2 (red line) sets of discharges for times in the middle of the interval used for MDB database compilation. As it is seen from Figure 6.1 the plasma in the S1 discharges

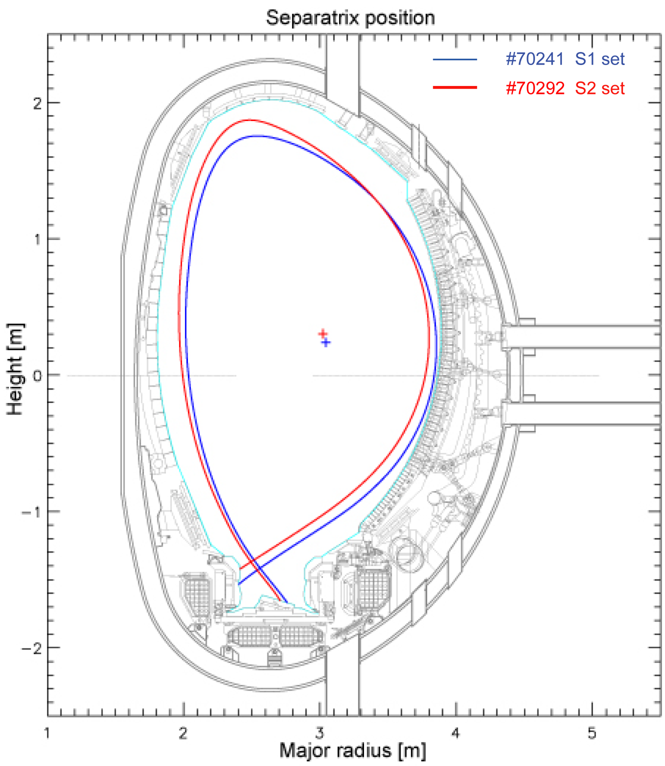

Figure 6.1: *Separatrix layout in S1 (blue) and S2 (red) regimes.*

is limited by poloidal midplane limiter and as a result, a rather thin scrape-off layer (SOL) can be expected. The strike point locations of both regimes differ with inner strike point of S2 shot being shifted upwards compared to S1 discharge. The upwards shifted inner strike point is necessary to achieve higher triangularity of plasma shape in S2. These examples of EFIT reconstruction represent well the whole set of S2 shots, which I considered here. But in S1 shots, the strike points cover relatively long path along the divertor surface (Figure 6.2). For better comparison the surface of divertor tiles is drawn. The Figure 6.2 shows the layout of strike points in divertor tiles for both regimes. It is clear that the evaluation of outer strike points location is wrong, unlike of inner strike points. This is probably caused by error of magnetic reconstruction using XLOC prucedure. The S2 plasmas shapes are almost the same with strike points located in the upper part of inner top divertor tile.

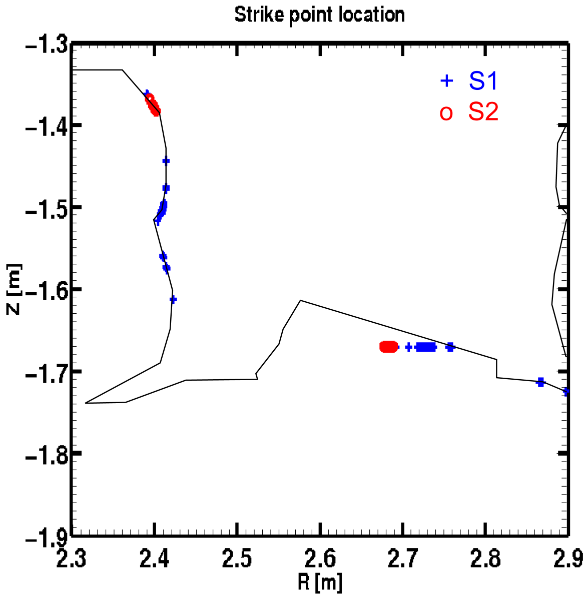

Figure 6.2: *Strike point locations in divertor region for both S1 and S2 discharges.*

6.2 Density and temperature profiles

As I mentioned before, LIDAR is a very clever system for measuring the electron temperature and density. The density and temperature profiles for both S1 and S2 regimes are shown in Figure 6.3. As it can be seen, the density is characterized by flat profiles in

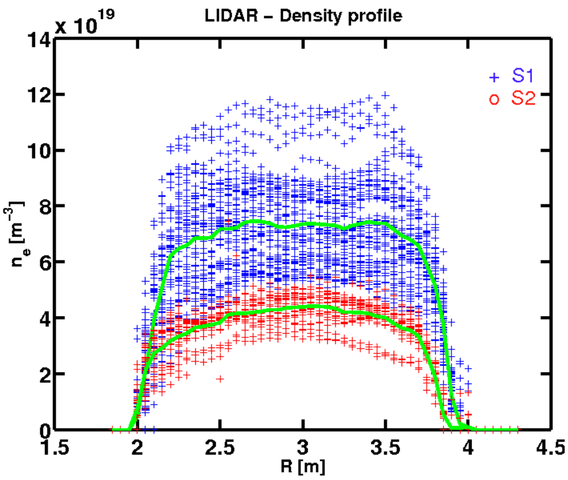

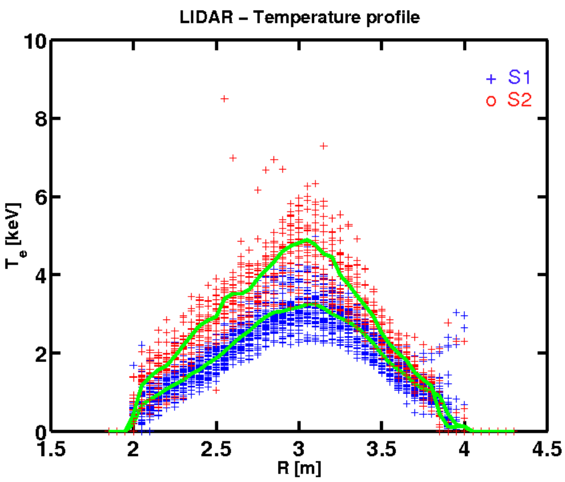

Figure 6.3: *LIDAR density (left) and temperarute (right) profiles measurement..*

both regimes, unlike the temperature. The S1 plasmas have almost twice higher density. Temperature exhibits more peaked profiles in S2, reaching almost twice higher central values compared to S1, as expected.
The next Figure 6.4 illustrates how the central electron temperature varies with total input power. It is clearly seen that the S1 discharges are composed from the two distinct groups: one with total input power of ∽ 9 MW and the second with total input power

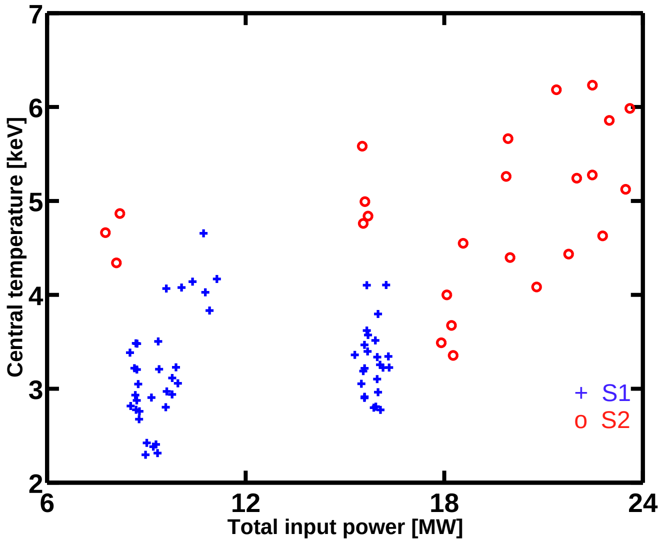

Figure 6.4: *Central electron temperature dependency on total input power.*

of $\backsim$ 16 MW. In agreement with Figure 6.3, it is seen that significantly higher central temperature on average is obtain in S2 regime reaching up to 6 keV in comparison with approximately 4 keV for S1 regime. The relation between central electron temperature and input power is not obvious, particularly in S1 regime.

6.3 Radiation pattern

A pure hydrogen plasma emits electromagnetic radiation. Microscopically this is caused due to the acceleration of the charged particles. The electrons are accelerated in two ways. Firstly they are accelerated by collisions, then the resulting radiation is called bremsstrahlung. Secondly they are subject to the acceleration of their cyclotron motion. The presence of impurities in the plasma produce energy losses through line radiation.
A measurement of the total radiation emitted from the plasma is important for evaluation of the energy balance. Power radiated fraction is a important characteristic especially in point of view of ITER. It is a ratio of total radiated power from plasma and the total input power into plasma. The radiated power fraction dependence on density is shown in Figure 6.5. As it can be seen the radiated power fraction in S1 regime increases linearly with density and reaches up to 70%, i.e. 70% of total input power is lost via radiation. On the other hand, the radiated power fraction for S2 regime is about 25%. The total radiated power found in divertor region as a function of density and of total input power is shown in Figure 6.6 (left panel). The S2 plasmas have lower density and hotter edges. And as it shown the S2 plasmas radiate less than the colder edges in S1 plasmas. The two S1 'clouds' correspond to the two groups of discharges in database which differ in amount of additional heating power. The divertor radiated power increases with density for S2 discharges. But for S1 shots, taking into account two distinct levels of input power, the divertor radiated power remains constant. Lower ability to radiate out the energy from the divertor in S2 regime without impurity seeding is apparent also in Figure 6.6 (right panel). Here, the dependence of divertor radiated power versus total input power is plotted.

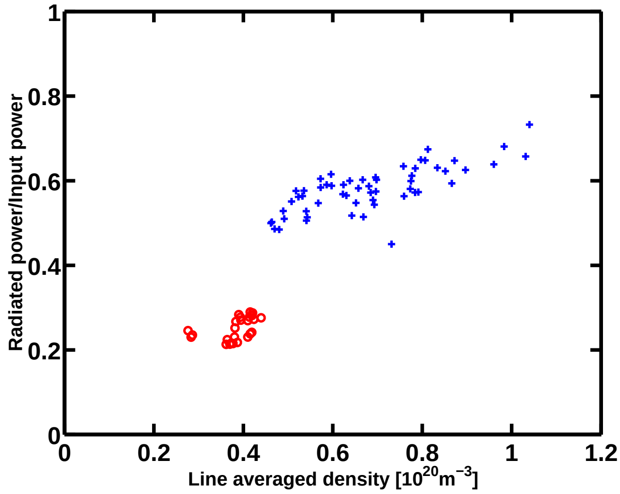

Figure 6.5: *Density dependance of radiated power fraction.*

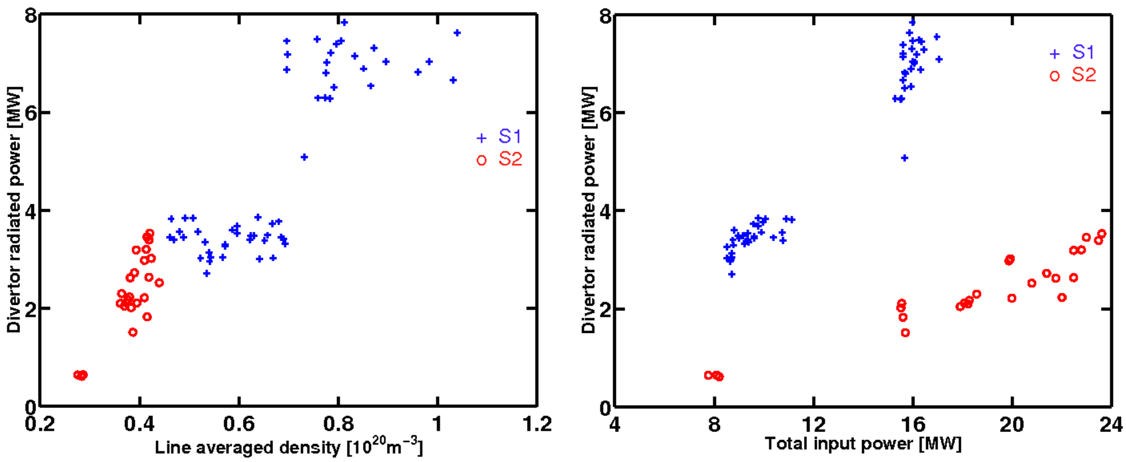

Figure 6.6: *Divertor radiated power as a function of density (left) and total input power (right).*

6.4 Impurities measurement

If the plasma is in direct contact with wall components, electrons and ions hit the surface. This particle bombardment leads to release of impurity atoms by collisions and for certain plasma facing materials by chemical reactions. In addition the wall material will be heated by the corresponding energy transfer. The incident plasma ions will be neutralized with a fraction of them being reflected. Neutralized particles entering the plasma are ionized again by electron impact or by charge exchange processes with plasma ions. Charge exchange processes in hot plasma regions will produce neutral particles at high energies, which can escape the plasma hitting also plasma facing components without direct plasma contact. The presence of the impurities may degrade severely the plasma properties necessary for nuclear fusion.

Fusion plasma consists of several ion species, which are ionized in the plasma. Therefore it is defined a quantity called effective charge Z_{eff}, which indicates how the plasma is 'dirty':

$$Z_{eff} = \frac{\sum n_j {Z_j}^2}{\sum n_j Z_j} \tag{6.1}$$

The Figure 6.7 (left) shows the measured Z_{eff} as a function of density. A visible spectroscopy (KS3 - vertical line of sight) is used for measuring the effective charge Z_{eff}. The S2 plasmas produce more impurities due to its low densities and therefore hotter edges, i.e. higher wall interaction and strain of plasma facing components. Because the plasma

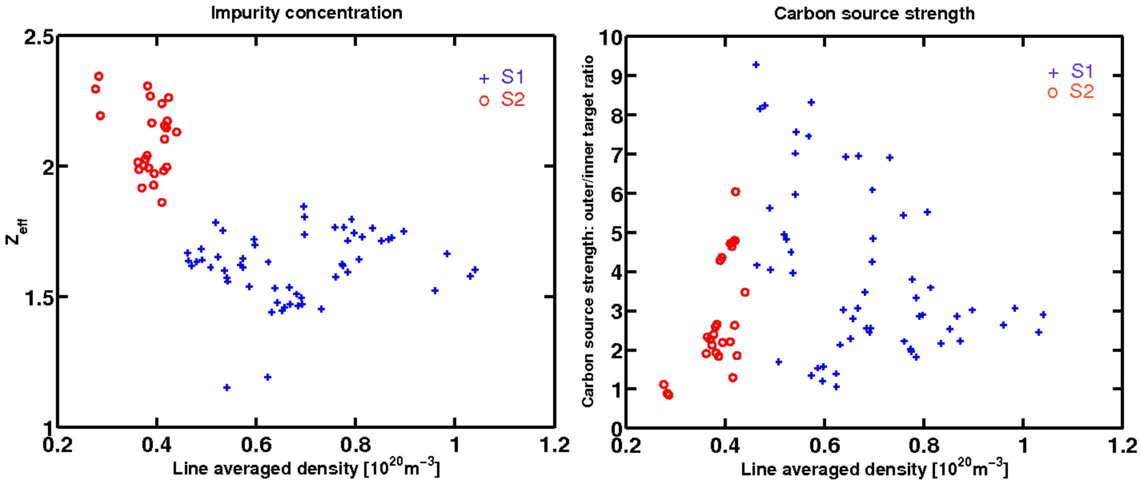

Figure 6.7: *Impurity concentration (left) and carbon source strength (right).*

facing components on JET are mainly made by carbon, I especially analyzed the ratios of CIII/Dalpha emission in the inner and outer divertor. This is an indicator of the carbon source strength, since it gives an idea of number of carbons released per incident neutral. The Figure 6.6 (right) shows the ratio of carbon source strength in the outer and inner divertor target. It is evident that the carbon production is much higher in outer divertor and the outer and inner ratio range varies from 1 to 9. No particular dependence of this ratio on density is observed.

6.5 Langmuir probes measurement

I analyzed the electron density profiles measured in SOL of JET tokamak by divertor Langmuir probes in both S1 and S2 regimes. Electron density profiles in SOL measured by divertor Langmuir probes (LPs) are shown in Figure 6.8 (S1 set left, S2 set right). I used different shots to represent S1 regime, because the advanced post discharge analysis of data from Langmuir probes measurements was not done for the series of S1 discharges discussed in previous sections. For S2 regime the same set of shots as before was used. Here, the seven JET discharges 66102-66108 were used to represent S1 regime. These were performed during a single experimental session High Ip at high delta - New ITER Shape on 25.4.2006. These S1 shots are characteristic by high plasma current of 2.5 MA and presence of compound ELMs activity with ELMs frequency varied on a shot to shot basis from 80 - 130 Hz.

Each data point in Figure 6.8 represents the evaluated output of the single or triple Langmuir probe averaged over the time window of 0.5 s. The y axis (density) is in logarithmic scale. The distance from separatrix mapped to mid-plane (RMPLP) is plotted on the x axis. The measured data are fitted by exponential. Only the data points plotted by blue or red colour are included into the fit. The black data points were excluded from the fit because they were measured either in the divertor region or they were rejected because of too low value and noisy character. The later case applies mostly to the S2 set of discharges. Note a rather good coverage of SOL density profile by divertor Langmuir

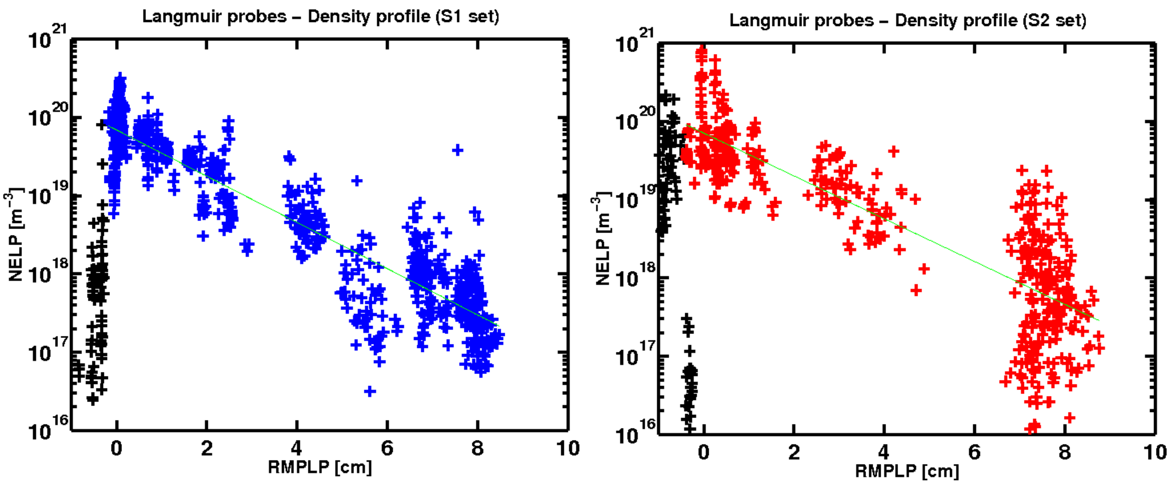

Figure 6.8: *Langmuir probes - density profile of SOL in both S1 (left) and S2 (right) sets of discharges. The fit by exponential is plotted by green line. Only the data points plotted by blue or red are used for fitting.*

probes for S1 set of shots. The best fit of S1 and S2 data, in the least squares sense, was obtained by formulas:

$$\text{S1:} \qquad n_e = 6.87 \cdot e^{-0.679r} \qquad [10^{19} m^{-3}]$$

$$\text{S2:} \qquad n_e = 7.05 \cdot e^{-0.629r} \qquad [10^{19} m^{-3}]$$

The coverage of SOL by divertor Langmuir probes in S2 set of discharges is rather worse. The reason of this may be be the difference in geometry (see Figure 6.1). I assume that the Langmuir probe measurements are hampered by radio frequency heating and current drive ICRH and LH applied during these shots. For fitting of S2 SOL density profiles, I did not take in account the data points in the range NELP$\in (0, 10^{19})$ taken close to separatrix. These points do not correspond to a specific shots, but for each shot, several points of the profile fall into this 'cloud'. I considered these measurements as wrongly evaluated output of Langmuir probes. Further decrease of data spread could be obtained by excluding Langmuir probe data measured during ELMs, where the evaluation of I-V characteristics fails or is affected by very large errors.

The electron density at separatrix is about the same for both S1 and S2 regimes reaching approximately $n_e = 7 \cdot 10^{19} m^{-3}$. In both cases, the profile can be well approximated by exponential. The decrease of electron density profile in SOL is faster for S1 regime, so the SOL in S1 appears to be slightly thinner compared to S2 set of discharges. This can be explained by smaller outer gap configuration of S1 set of shots compared to the S2 set (see Figure 6.1).

Summary

This thesis gives an overview of comparison of the basic plasma parameters in various regimes of the JET tokamak. First regime is called the ELMing H-mode (S1), which exhibits a transport barrier at the plasma edge and periodic relaxations of edge pressure profile (ELMs). The second one is characterized by Internal Transport Barrier (ITB) in plasma core (S2) and is a key to non-inductive, steady-state operation of future devices.

A brief introduction into the physics of magnetically confined plasma is given in Chapter 1. The outline of basic components and principles of operation of tokamak device is summarized in Chapter 2. Followings Chapters 3 and 4 give an overview of JET tokamak, its operating regimes and its available diagnostics. Some of the JET diagnostics are described in more detail. Description and example of application of MDB database creation tool is presented in Chapter 5. The results obtained are summarized within Chapter 6.

In order to compare the both operating regimes a set of 23 discharges performed in S1 regime and 10 discharges to represent S2 regime were selected. More than 80 relevant quantities including plasma geometry, basic plasma parameters, profiles of electron temperature T_e, density n_e, ion temperature T_i, and all edge and scrape-off layer (SOL) properties which are currently measured on JET, were used to characterize these two regimes. The proper time windows, where the main plasma parameters are stationary for each discharge, were selected. For each time window, the mean values of the evaluated quantities were computed and stored using the MDB database creation tool.

The plasma geometry is very reproducible within the S2 set of discharges featuring the inner strike points placed high onto the inner top divertor tile. On the other hand, large spread of strike point locations is observed for S1 set of pulses. Further, it was found out that the outer strike points seem to be wrongly evaluated by XLOC procedure being placed significantly bellow the divertor surface. This problem calls for further attention and investigation.

The density is characterized by flat profiles in both regimes. S1 regime operates with about two times higher density compared to S2. Temperature exhibits more peaked profiles in S2, reaching almost twice as high central values compared to S1.

Radiated power fraction in S1 regime increases linearly with density and reaches up to 70%. On the contrary, the radiated power fraction for S2 regime without seeding of extrinsic impurities is only about 25%. This finding is extremely important with respect to ITER as advanced ITER regimes with only 25% of radiated power fraction would mean unacceptably high heat loads to the divertor structure.

Impurity content was characterized by the effective charge Z_{eff} for both regimes. It was found that impurity content of the S2 pulses is higher due to the hotter edge plasmas, i.e. higher plasma-wall interaction and strain of the plasma facing components. The carbon production rate is much higher in the outer divertor with the ratio of outer to inner being from 1 to 9. No particular dependence of this ratio on density was observed.

The SOL electron density profiles, measured by divertor Langmuir probes, were analysed for both S1 and S2 regimes. The electron density at separatrix is about the same for both S1 and S2 regimes reaching approximately $n_e = 7 \cdot 10^{19} m^{-3}$. In both cases, the profile can be well approximated by exponential.

In conclusion, it was found that for ITER advanced regimes, additional extrinsic impurity seeding or further increase of density in divertor is needed in order to increase radiation power fraction and as a result to keep the power loads on divertor targets sufficiently low.

It is necessary to stress that these thesis contains only the basic comparison of some main plasma parameters for a very limited number of JET pulses. Gradual inclusion of significantly more JET pulses into the database accompanied with more detailed analysis of its physics content is envisaged for the future.

References

[1] J. Wesson: The Science of JET, JET-R(99)13.

[2] F.F. Chen: Introduction to Plasma Physics and Controlled Fusion, vol. 1, New York : Plenum Press, 2006.

[3] IPP Summer University for Plasma Physics, September 26 - 30, 2005, Greifswald, Germany

[4] J. Wesson: Tokamaks, 3rd ed., Oxford Univ. Press, 2004.

[5] J. Mlynar: Focus on: JET, EFD-R(07)01.

[6] R.C. Wolf: Internal transport barriers in tokamak plasmas, Plasma Phys. Control. Fusion **45** (2003) R1-R91

[7] I.H. Hutchinson: Principles of plasma diagnostics, Cambridge University Press, 2001.

[8] A.J.H. Donné: Introduction to plasma Diagnostics, Fusion Science and Technology **45** T2, 383-390, 2004.

Images courtesy: EFDA-JET, Max-Planck-Institut für Plasmaphysic

Web page: http://users.jet.efda.org